Seven-co-ordination in Metal Complexes of Quinquedentate Macrocyclic Ligands. Part IV.[1] Crystal and Molecular Structures of Two Pentagonal Bipyramidal Iron(II) Complexes

By **Michael G. B. Drew*** and **A. Hamid bin Othman**, Department of Chemistry, The University, Whiteknights, Reading RG6 2AD
S. Martin Nelson,* Department of Chemistry, Queen's University, Belfast BT9 5AG

The crystal structures of two iron(II) complexes of stoicheiometry [FeL(NCS)$_2$], where L is a 15- or 16-membered 'N$_5$' macrocycle, have been determined. Crystals of (I) (L = $C_{15}N_5H_{23}$) are triclinic with a = 12.923(11), b = 7.165(9), c = 11.673(8) Å, α = 93.24(11), β = 90.75(11), γ = 110.40(12)°, Z = 2, space group $P\bar{1}$. Crystals of (II) (L = $C_{16}N_5H_{25}$) are monoclinic, space group $P2_1/c$ with a = 7.746(8), b = 11.747(12), c = 24.367(18) Å, β = 102.08(12)°, Z = 4. The two structures were solved by Patterson and Fourier methods from 1 057 and 1 131 independent reflections above background collected by counter methods and refined to R 0.058 and 0.060, respectively. In both structures, the metal atoms have distorted pentagonal bipyramidal environments with the thiocyanate ligands in axial positions and the five nitrogen atoms of the macrocycle in equatorial positions. The Fe–N bond lengths and the conformations of the girdles are different in the two molecules as a consequence of the extra CH$_2$ group in (II). However, both molecules have similar structures to those of the analogous Fe^{III} cations.

IN Part III we described the preparation and properties of a number of seven-co-ordinate iron(II) complexes of the types [FeLX$_2$], [FeLX(H$_2$O)]X·xH$_2$O, and [FeL(H$_2$O)$_2$]X·ClO$_4$; where X = halide or pseudohalide and L represents the 15- and 16-membered macrocycles L^1 and L^2. In order further to define the molecular geometries of these complexes and to compare them with those of the previously investigated Fe^{III} derivatives,[2] we have determined the crystal and molecular structures of two members of the series, FeL^1(NCS)$_2$ (I) and FeL^2(NCS)$_2$ (II), and these are reported in the present paper. The structure of [FeL^1(H$_2$O)$_2$][Cl,ClO$_4$] is reported elsewhere.[3] Of particular interest were the effects of metal-ion size and electron configuration on the conformation of the co-ordinated macrocycle. We also wished to gain further insight into certain of the physical properties, particularly the electronic spectra, described in Part III. A preliminary report of this work has been published.[4]

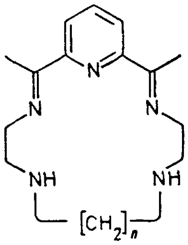

L^1, n = 2
L^2, n = 3

EXPERIMENTAL

Crystals were prepared as described previously.[1]

Crystal Data (I).—$C_{17}H_{23}N_7S_2Fe$, M = 445.43, Triclinic, a = 12.923(11), b = 7.165(9), c = 11.673(8)Å, α = 93.24(11), β = 90.75(11), γ = 110.40(12)°, U = 1 010.8 Å^3, D_c = 1.46, Z = 2, D_m = 1.45(2), F(000) = 464. Space group $P\bar{1}$ from the successful structure determination. Mo-K_α radiation, λ = 0.7107 Å; μ(Mo-K_α) = 9.2 cm^{-1}.

(II). $C_{18}H_{25}N_7S_2Fe$, M = 459.43, Monoclinic, a = 7.746(8), b = 11.747(12), c = 24.367(18) Å, β = 102.08(12)°, U = 2 166.8 Å^3, D_c = 1.37, Z = 4, D_m = 1.37(2), F(000) = 960. Space group $P2_1/c$ from systematic absences: $h0l$, $l = 2n + 1$ and $0k0$, $k = 2n + 1$. μ(Mo-K_α) = 7.5 cm^{-1}.

The majority of crystals of (I) were twinned with $hk0$ common, but with some difficulty an untwinned crystal was obtained. Crystals with dimensions *ca.* 0.60 × 0.15 × 0.25 mm (I) and *ca.* 0.2 × 0.25 × 0.44 mm (II) were both mounted with a^* parallel to the instrument axis of a General

---

[1] Part III, M. G. B. Drew, J. Grimshaw, P. D. A. McIlroy, and S. M. Nelson, *J.C.S. Dalton*, preceding paper.

[2] M. G. B. Drew, A. H. Othman, P. D. A. McIlroy, and S. M. Nelson, *J.C.S. Dalton*, 1975, 2507.

[3] M. G. B. Drew, A. H. Othman, P. D. A. McIlroy, and S. M. Nelson, *Acta Cryst.*, 1976, **B32**, 1029.

[4] M. G. B. Drew, A. H. Othman, W. E. Hill, P. D. A. McIlroy, and S. M. Nelson, *Inorg. Chim. Acta*, 1975, **12**, L25.

Electric XRD 5 apparatus which was used to measure diffraction intensities and cell dimensions (*via* least-squares refinement of several high-angle reflections). It was equipped with a manual goniostat, scintillation counter, and pulse-height discriminator. Zirconium-filtered molybdenum *X*-radiation was used and the stationary-crystal–stationary counter method employed to measure 1 991 (I) and 1 784 (II) independent reflections with $2\theta < 40°$, counts being taken for 10 s. Individual backgrounds were taken for those reflections whose counts were seriously affected by the streaking of other orders. For other reflections, backgrounds were taken from plots of background as a function of 2θ. Several standard reflections were measured during the course of both experiments but no significant changes in intensity were observed. No absorption or extinction corrections were applied. The standard deviations $\sigma(I)$ of the reflections were taken to be $[I + 2E + (0.03I^2)]^{\frac{1}{2}}$ where E is the estimated background of the reflection. 1 057 (I) and 1 131 (II) reflections with $I > \sigma(I)$ were used in subsequent calculations.

Structure Determination.—For both (I) and (II), the positions of the iron atoms were determined from a Patterson function and Fourier syntheses were then calculated to determine the remaining atom positions. Both structures were refined by full-matrix least squares with the non-hydrogen atoms given anisotropic thermal parameters of the form $\exp-[2\pi^2\sum_i\sum_j(h_ih_jb_ib_jU_{ij})]$; $i,j = 1,2,3$ where b_i is the ith reciprocal cell parameter. The non-methyl hydrogen atoms were given positions calculated assuming tetrahedral or trigonal geometry; these corresponded to positive regions in the difference-Fourier map and were included in the structure-factor calculation but not refined. Hydrogen atoms were given isotropic thermal parameters of the form $\exp(-8\pi^2U\sin^2\theta/\lambda^2)$ with individual values set equal to those of the atom to which they were bonded. The weighting scheme, chosen to give average values of $w\Delta^2$ for groups of reflections, independent of F_o and $\sin\theta/\lambda$, was $\sqrt{w} = 1$ for $F_o < F^*$ and $\sqrt{w} = F^*/F_o$ for $F_o > F^*$. F^* was 37 in (I) and 55 in (II). Calculations were made on a CDC 7600 computer at the University of London Computer Centre with programs described in ref. 5. Atomic scattering factors

TABLE 1

Atomic co-ordinates ($\times 10^4$) for (I), with estimated standard deviations in parentheses

	x	*y*	*z*
Fe	2 490(2)	0 044(3)	2 580(2)
S(1)	6 114(3)	4 698(7)	1 924(4)
S(2)	−1 153(3)	−4 826(7)	1 602(4)
N(1)	4 009(11)	2 522(18)	2 580(9)
N(2)	0 985(11)	−2 360(18)	2 308(11)
C(1)	4 897(12)	3 453(22)	2 263(11)
C(2)	0 118(13)	−3 407(20)	1 993(12)
N(3)	1 991(8)	1 502(15)	1 084(8)
C(4)	0 926(10)	1 808(24)	1 294(12)
C(5)	1 045(11)	2 836(21)	2 448(13)
N(6)	1 501(8)	1 896(16)	3 255(9)
C(7)	1 408(10)	2 089(19)	4 294(15)
C(8)	1 920(11)	0 995(18)	5 116(13)
N(9)	2 468(8)	0 007(16)	4 427(9)
C(10)	2 954(12)	−1 080(22)	4 996(12)
C(11)	3 541(11)	−2 108(20)	4 162(15)
N(12)	3 471(9)	−1 797(16)	3 139(11)
C(13)	3 977(11)	−2 696(21)	2 270(13)
C(14)	4 073(11)	−1 586(21)	1 188(13)
N(15)	3 019(8)	−1 301(16)	0 967(9)
C(16)	3 035(12)	−0 133(23)	−0 034(11)
C(18)	1 994(13)	0 418(25)	−0 013(12)
C(20)	0 825(13)	3 381(24)	4 945(13)
C(21)	1 881(16)	0 960(26)	6 271(14)
C(22)	2 330(21)	−0 226(35)	6 822(14)
C(23)	2 904(16)	−1 252(31)	6 194(17)
C(24)	4 168(14)	−3 358(22)	4 733(14)

TABLE 2

Atomic co-ordinates ($\times 10^4$) for (II), with estimated standard deviations in parentheses

	x	*y*	*z*
Fe	−0 335(2)	2 668(2)	1 288(1)
S(1)	3 875(5)	3 646(4)	3 030(2)
S(2)	−4 337(6)	1 955(5)	−0 500(2)
C(2)	−3 230(20)	2 169(13)	0 129(7)
N(1)	1 725(15)	3 028(10)	2 005(5)
N(2)	−2 392(16)	2 340(13)	0 585(6)
C(1)	2 591(17)	3 298(12)	2 441(6)
N(3)	−1 247(14)	1 265(9)	1 867(4)
N(6)	−2 426(13)	3 490(10)	1 679(4)
N(9)	−0 469(13)	4 535(9)	1 115(4)
N(12)	1 601(14)	3 170(9)	0 746(4)
N(15)	0 745(17)	0 983(10)	0 989(5)
C(4)	−2 150(19)	1 838(13)	2 266(6)
C(5)	−3 386(18)	2 692(13)	1 972(6)
C(7)	−2 820(17)	4 537(12)	1 602(6)
C(8)	−1 643(17)	5 179(12)	1 309(5)
C(10)	0 649(16)	5 027(11)	0 839(5)
C(11)	1 864(19)	4 208(12)	0 650(6)
C(13)	2 631(18)	2 254(14)	0 563(6)
C(14)	1 437(22)	1 199(14)	0 485(6)
C(16)	1 827(28)	0 295(17)	1 390(8)
C(17)	0 835(21)	−0 313(14)	1 796(7)
C(18)	0 145(19)	0 519(13)	2 167(6)
C(20)	−4 376(19)	5 129(14)	1 796(7)
C(21)	−1 730(20)	6 365(13)	1 233(6)
C(22)	−0 572(25)	6 835(13)	0 948(7)
C(23)	0 667(21)	6 180(13)	0 755(6)
C(24)	3 319(17)	4 648(14)	0 334(6)

TABLE 3

Molecular dimensions for (I) and (II)

(*a*) Bond lengths (Å)	(I)	(II)
Fe–N(1)	2.140(11)	2.146(11)
Fe–N(2)	2.106(11)	2.119(12)
Fe–N(3)	2.280(11)	2.370(11)
Fe–N(6)	2.259(13)	2.259(11)
Fe–N(9)	2.159(11)	2.232(11)
Fe–N(12)	2.239(13)	2.274(12)
Fe–N(15)	2.287(12)	2.323(13)
N(1)–C(1)	1.186(18)	1.175(18)
N(2)–C(2)	1.151(18)	1.179(20)
C(1)–S(1)	1.583(15)	1.619(14)
C(2)–S(2)	1.645(14)	1.612(16)
N(3)–C(4)	1.488(19)	1.474(20)
C(4)–C(5)	1.478(21)	1.466(19)
C(5)–N(6)	1.422(21)	1.471(19)
N(6)–C(7)	1.226(21)	1.270(18)
C(7)–C(20)	1.556(24)	1.550(22)
C(7)–C(8)	1.551(23)	1.480(20)
C(8)–N(9)	1.397(20)	1.342(17)
N(9)–C(10)	1.353(22)	1.336(17)
C(8)–C(21)	1.350(23)	1.405(20)
C(21)–C(22)	1.367(35)	1.362(25)
C(22)–C(23)	1.400(36)	1.389(25)
C(23)–C(10)	1.411(25)	1.366(20)
C(10)–C(11)	1.546(24)	1.487(20)
C(11)–C(24)	1.569(26)	1.579(21)
C(11)–N(12)	1.236(22)	1.265(18)
N(12)–C(13)	1.452(20)	1.464(20)
C(13)–C(14)	1.514(23)	1.535(23)
C(14)–N(15)	1.467(20)	1.461(21)
N(15)–C(16)	1.471(19)	1.402(22)
C(16)–C(17)		1.549(28)
C(16)–C(18)	1.529(26)	
C(17)–C(18)		1.502(23)
C(18)–N(3)	1.461(18)	1.461(17)

---

[5] ' *X*-Ray ' system of programs, ed. J. M. Stewart, University of Maryland Technical Report, TR 192, version of July 1970.

TABLE 3 (*Continued*)

(*b*) Angles (°)	(I)	(II)
N(1)–Fe–N(2)	171.3(5)	179.0(5)
N(1)–Fe–N(3)	84.2(4)	85.2(4)
N(1)–Fe–N(6)	94.4(5)	92.9(4)
N(1)–Fe–N(9)	94.2(4)	87.6(4)
N(1)–Fe–N(12)	87.8(5)	87.3(4)
N(1)–Fe–N(15)	88.8(4)	99.6(4)
N(2)–Fe–N(3)	88.4(4)	95.0(5)
N(2)–Fe–N(6)	87.6(5)	86.2(5)
N(2)–Fe–N(9)	94.5(4)	91.6(5)
N(2)–Fe–N(12)	95.8(5)	93.0(5)
N(2)–Fe–N(15)	84.8(4)	81.4(5)
N(3)–Fe–N(6)	71.2(4)	73.6(4)
N(3)–Fe–N(9)	142.1(5)	142.0(4)
N(3)–Fe–N(12)	145.9(4)	147.2(4)
N(3)–Fe–N(15)	74.6(4)	76.5(4)
N(6)–Fe–N(9)	71.1(4)	69.6(4)
N(6)–Fe–N(12)	142.7(4)	138.7(4)
N(6)–Fe–N(15)	145.1(4)	146.4(4)
N(9)–Fe–N(12)	71.5(5)	69.2(4)
N(9)–Fe–N(15)	143.4(5)	141.5(4)
N(12)–Fe–N(15)	72.1(4)	73.4(4)
Fe–N(1)–C(1)	156.1(11)	167.3(12)
Fe–N(2)–C(2)	165.1(13)	164.8(14)
N(1)–C(1)–S(1)	176.2(13)	177.1(14)
N(2)–C(2)–S(2)	176.4(16)	178.6(16)
Fe–N(3)–C(4)	111.0(8)	108.4(8)
Fe–N(3)–C(18)	111.8(10)	115.7(9)
C(4)–N(3)–C(18)	113.2(10)	110.2(10)
N(3)–C(4)–C(5)	106.3(10)	109.9(12)
C(4)–C(5)–N(6)	110.8(13)	109.2(11)
Fe–N(6)–C(5)	118.0(9)	114.3(8)
Fe–N(6)–C(7)	118.9(11)	121.5(10)
C(5)–N(6)–C(7)	123.0(14)	123.9(12)
N(6)–C(7)–C(8)	119.9(14)	114.4(12)
N(6)–C(7)–C(20)	127.6(15)	124.6(13)
C(8)–C(7)–C(20)	112.5(14)	121.0(12)
C(7)–C(8)–C(21)	129.2(16)	123.5(13)
C(7)–C(8)–N(9)	106.4(13)	114.2(12)
N(9)–C(8)–C(21)	124.5(16)	122.2(13)
Fe–N(9)–C(10)	121.2(10)	120.8(9)
Fe–N(9)–C(8)	123.7(10)	119.8(9)
C(8)–N(9)–C(10)	115.1(12)	119.3(11)
N(9)–C(10)–C(23)	123.3(17)	122.2(13)
C(11)–C(10)–C(23)	125.5(17)	124.6(13)
N(9)–C(10)–C(11)	111.2(13)	113.2(11)
C(8)–C(21)–C(22)	119.4(19)	116.6(14)
C(21)–C(22)–C(23)	119.4(17)	121.7(15)
C(22)–C(23)–C(10)	118.1(20)	117.9(15)
C(10)–C(11)–N(12)	115.4(15)	115.5(13)
C(10)–C(11)–C(24)	115.8(14)	120.0(12)
N(12)–C(11)–C(24)	128.8(15)	124.5(13)
Fe–N(12)–C(11)	120.5(11)	120.6(10)
Fe–N(12)–C(13)	118.7(10)	117.0(9)
C(11)–N(12)–C(13)	120.7(14)	122.1(13)
N(12)–C(13)–C(14)	108.8(13)	106.2(12)
C(13)–C(14)–N(15)	108.1(11)	110.6(12)
C(14)–N(15)–C(16)	113.1(11)	114.5(13)
Fe–N(15)–C(16)	111.8(9)	118.3(11)
Fe–N(15)–C(14)	110.5(8)	109.7(9)
N(15)–C(16)–C(1*x*) *	107.3(11)	114.0(16)
C(16)–C(17)–C(18)		111.7(14)
C(1*y*) *–C(18)–N(3)	108.2(11)	114.0(11)

* *x* Is 7 in (II), 8 in (I); *y* is 6 in (I), 7 in (II).

for non-hydrogen atoms were taken from ref. 6, and for hydrogen from ref. 7. Corrections for the real and imaginary part of the anomalous dispersion for iron and sulphur were also taken from ref. 6. Final *R* values were 0.058 (I) and 0.060 (II) for the 1 057 and 1 131 observed reflections. For both (I) and (II) subsequent difference-Fourier maps showed no significant peaks. In the final cycles of refinement no shift was $> 0.05\sigma$. The reflections given zero weight showed no large discrepancies. Final positional parameters for (I) and (II) are given in Tables 1 and 2. Molecular dimensions for the structures are compared in Table 3. Observed and calculated structure factors, thermal parameters, and intermolecular contacts <3.75 Å for both (I) and (II) are listed in Supplementary Publication SUP 21659 (12 pp., 1 microfiche).*

DISCUSSION

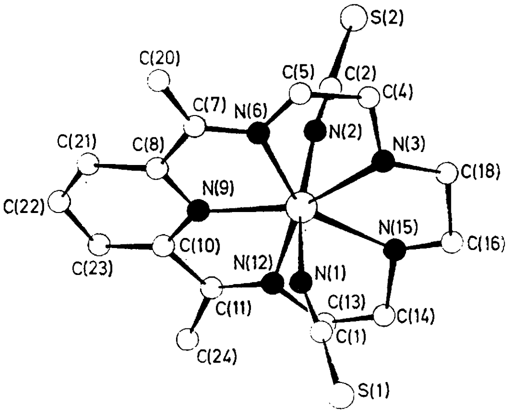

FIGURE 1 (I)

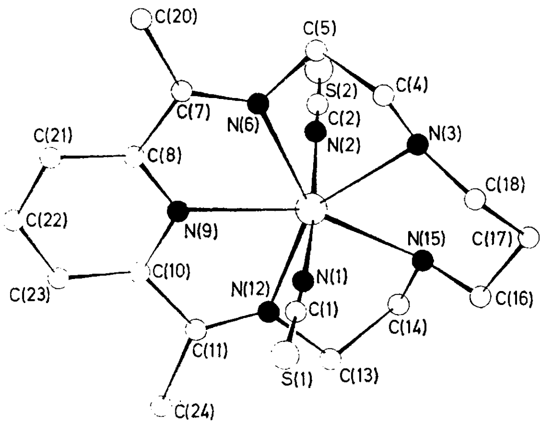

FIGURE 2 (II)

The two molecules are shown in Figures 1 and 2 together with the atom numbering scheme used in the analyses. The co-ordination polyhedra of the two molecules are approximately pentagonal bipyramidal as found previously [2] for the two corresponding iron(III) compounds $[Fe(L^1NCS)_2]ClO_4$, (III) and $[FeL^2(NCS)_2]ClO_4$, (IV), the five nitrogen atoms of the macrocycle lying approximately in an equatorial plane containing the metal atom, and the thiocyanate ligands in axial positions.

The conformations of the macrocycles L^1 in (I) and L^2 in (II) are characterised by the least-squares planes (Table 4) and the torsion angles (Table 5). The conformations of L^1 in (I) and (III) are very similar as are those of L^2 in (II) and (IV). Thus in (I), the ten *cis*-angles involving N(1) and N(2) are within 6° of 90°. The maximum

---

* See Notice to Authors No. 7 in *J.C.S. Dalton*, 1975, Index issue.

[6] 'International Tables for *X*-Ray Crystallography,' vol. III, Kynoch Press, Birmingham, 1962.

[7] R. F. Stewart, E. R. Davidson, and W. T. Simpson, *J. Chem. Phys.*, 1965, **42**, 3175.

deviation of an atom from the FeN_5 least-squares plane is 0.12 Å, a value equivalent to that in (III). The deviations from the plane of all atoms in the molecule show the same C_2 distortion as in (III). A similar pattern is found [3] in $[FeL^1(H_2O)_2]^{2+}$, in which the cation has crystallographically imposed C_2 symmetry.

TABLE 4

Least-squares planes calculations for (I) and (II) in the form $Ax + By + Cz = D$, where x,y,z are the crystallographic fractional co-ordinates of the atoms. Distances (Å) of the relevant atoms from each plane are given in square brackets

Plane (1): Fe, N(1), C(1), S(1)

	A	B	C	D
(I):	7.10	−4.30	8.56	3.95
(II):	1.39	10.77	−9.42	1.61

[(I): Fe 0.00, N(1) 0.01, C(1) −0.03, S(1) 0.01, C(7) −0.18, C(8) 1.36, N(15) −0.43, C(14) 0.63; (II): Fe 0.00, N(1) 0.00, C(1) 0.00, S(1) 0.00, N(6) 0.23, C(5) −1.04, C(13) 0.65, C(14) −0.58]

Plane (2): Fe, N(2), C(2), S(2)

	A	B	C	D
(I):	−6.46	2.89	9.57	0.87
(II):	−1.20	11.53	−1.91	2.87

[(I): Fe 0.00, N(2) 0.02, C(2) −0.03, S(2) 0.01, N(3) −0.69, C(4) 0.29, C(11) 0.21, N(12) −0.63; (II): Fe 0.00, N(2) 0.00, C(2) 0.00, S(2) 0.00, C(5) 0.26, N(12) 0.45, C(4) −0.93, C(13) −0.69]

Plane (3): Fe, N(3), N(6), N(9), N(12), N(15)

	A	B	C	D
(I):	7.89	3.77	0.18	2.03
(II):	4.62	1.79	15.71	2.33

[(I): Fe 0.00, N(3) −0.12, N(6) 0.08, N(9) 0.00, N(12) −0.08, N(15) 0.12, C(7) 0.06, C(8) 0.05, C(10) 0.02, C(11) −0.04, C(20) 0.02, C(21) 0.07, C(22) 0.16, C(23) 0.10, C(24) −0.07, C(4) 0.60, C(5) 0.10, C(13) −0.13, C(14) −0.60, C(16) −0.31, C(18) 0.30; II: Fe −0.02, N(3) −0.25, N(6) 0.19, N(9) −0.02, N(12) −0.15, N(15) 0.25, C(7) 0.30, C(8) 0.10, C(10) −0.19, C(11) −0.31, C(20) 0.62, C(21) 0.05, C(22) −0.12, C(23) −0.27, C(24) −0.56, C(4) −0.56, C(5) 0.31, C(13) −0.18, C(14) 0.69, C(16) −0.75, C(17) −0.82, C(18) −1.24]

Plane (4): N(9), C(8), C(10), C(21), C(22), C(23)

	A	B	C	D
(I):	7.87	3.74	0.76	2.29
(II):	3.76	1.44	18.13	2.50

[(I): N(9) −0.01, C(8) −0.02, C(10) 0.01, C(21) 0.03, C(22) −0.02, C(23) 0.00; (II): N(9) 0.00, C(8) 0.00, C(10) −0.01, C(21) 0.00, C(22) −0.01, C(23) 0.01]

Plane (5): Fe, N(3), N(6)

	A	B	C	D
(I):	7.78	3.76	1.08	2.23
(II):	4.31	3.59	15.56	2.82

[(I): C(4) −0.69, C(5) −0.09; (II): C(4) −0.44, C(5) 0.24]

Plane (6): Fe, N(12), N(15)

	A	B	C	D
(I):	7.72	3.90	−0.71	1.75
(II):	4.55	0.03	16.28	1.95

[(I): C(13) 0.10, C(14) 0.69; (II): C(13) −0.17, C(14) 0.51]

Plane (7): Fe, N(3), N(15)

	A	B	C	D
(I):	8.77	3.21	0.21	2.25
(II):	5.64	1.42	12.37	1.78

[(I): C(16) 0.37, C(18) −0.37; (II): C(16) −1.01, C(17) −0.86, C(18) −1.05]

Angles (°) between planes: (I): (1)–(2), 84.0, (3)–(4) 2.8; (II): (1)–(2) 24.2, (3)–(4) 8.0.

Variations in planarity for (II) are also the same as in (IV), the presence of the six-membered ring in (II) making larger distortions, with N(3) 0.25 below and N(15) 0.25 Å above the least-squares plane of FeN_5. Of the carbon atoms in the unsaturated part of the molecule, C(20) and C(24) are the farthest distance from the plane (0.62 and −0.56 Å). As a whole, the deviations are slightly less than in (IV), the corresponding Fe^{III} complex [C(20) 0.81, C(24) −0.78 Å], which suggests that the larger bond lengths from metal to N(3) and N(15) reduce the strain for the six-membered ring and hence decrease its effect on the rest of the macrocycle.

There is a small increase in the average Fe–N equatorial bond length from the Fe^{III} to the corresponding Fe^{II} complexes. This is the trend expected on the basis of the radii of the metal ions. However, the effect is small [*ca.* 0.02 Å in (I), and 0.03 Å in (II)], appreciably less than the difference (0.12 Å) in Pauling radii.[8] The smallness of the effect can no doubt be accounted for in terms of the cyclic nature of the quinquedentate ligand which cannot respond freely to change in metal-ion size. This small increase in mean equatorial Fe–N bond length can be compared with the mean increase in axial Fe–N(NCS) bond length of 0.13 Å. Here of course there is no comparable macrocycle constraint, and the bond lengths reflect variations in ion size.

TABLE 5

Torsion angles (°) in the three saturated rings of (I) and (II) *

	(I)	(II)
Fe–N(6)–C(5)–C(4)	22.6	38.4
N(6)–C(5)–C(4)–N(3)	−47.0	−55.8
C(5)–C(4)–N(3)–Fe	51.0	45.2
C(4)–N(3)–Fe–N(6)	−29.9	−18.3
N(3)–Fe–N(6)–C(5)	4.0	−10.5
Fe–N(12)–C(13)–C(14)	20.4	33.0
N(12)–C(13)–C(14)–N(15)	−45.6	−52.6
C(13)–C(14)–N(15)–Fe	50.6	47.3
C(14)–N(15)–Fe–N(12)	−29.9	−21.6
N(15)–Fe–N(12)–C(13)	4.6	−7.4
Fe–N(15)–C(16)–C(1x) †	−42.9	71.2
N(15)–C(16)–C(17)–C(18)		−66.2
N(15)–C(16)–C(18)–N(3)	57.0	
C(16)–C(17)–C(18)–N(3)		66.9
C(1y)†–C(18)–N(3)–Fe	−43.6	−70.9
C(18)–N(3)–Fe–N(15)	15.8	52.9
N(3)–Fe–N(15)–C(16)	15.6	−54.7

* Torsion angles are of opposite signs to those in ref. 3 but, as all four unit cells are centrosymmetric and therefore contain both enantiomorphs, they are strictly comparable. † $x = 8$ in (I) and 7 in (II); $y = 6$ in (I) and 7 in (II).

However, closer inspection of the equatorial Fe–N bond lengths in the corresponding Fe^{II} and Fe^{III} complexes reveals a consistent pattern in that some of the bond distances actually decrease on reduction of Fe^{III} to Fe^{II}. The changes in individual Fe–N bond lengths are given in Table 6. Considering the two macrocycles of L^1 first, it can be seen that while a change in metal oxidation state of +3 to +2 leads to substantial increase (0.068 and 0.063 Å) in the lengths of the bonds from metal to the two saturated nitrogens [N(3) and N(15)], there is no change in the distances to the two imino-nitrogens [N(6) and N(12)], and there is a significant decrease (0.04 Å) in the distance to the pyridine nitrogen, N(9). Thus we have an ordering of Fe–N distances of Fe–N(pyridine) < Fe–N(imino) < Fe–N(saturated) in the Fe^{II} complex,

---

[8] L. Pauling, ' The Nature of the Chemical Bond,' 3rd edn., Cornell University Press, Ithaca, New York, 1960.

TABLE 6

Fe–N bond lengths (Å) in compounds (I)—(IV), and differences (Δ) between them

Macrocycle L^1	(I)	(III)	Δ
Fe–N(3)	2.280(11)	2.212(15)	0.068
Fe–N(6)	2.259(13)	2.259(13)	0.000
Fe–N(9)	2.159(11)	2.198(13)	−0.039
Fe–N(12)	2.239(13)	2.248(13)	−0.009
Fe–N(15)	2.287(12)	2.224(15)	0.063
Macrocycle L^2	(II)	(IV)	
Fe–N(3)	2.370(11)	2.309(12)	0.061
Fe–N(6)	2.259(11)	2.237(13)	0.022
Fe–N(9)	2.232(11)	2.251(10)	−0.019
Fe–N(12)	2.274(11)	2.228(11)	0.046
Fe–N(15)	2.323(13)	2.268(12)	0.055
Differences in bond lengths between macrocycles			
Fe–N(3)	0.090	0.097	
Fe–N(6)	0.000	−0.022	
Fe–N(9)	0.073	0.053	
Fe–N(12)	0.035	−0.020	
Fe–N(15)	0.036	0.042	

while in the Fe^{III} complex the order of the two last-mentioned bond types is reversed.

A similar pattern is observed for the two complexes of macrocycle L^2, though the effect is smaller and in addition there is a slight increase of (0.022 and 0.046 Å) in the Fe–N(imino) bond lengths from +3 to +2.

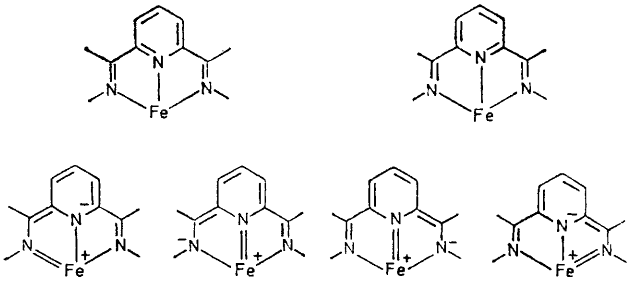

In Part III [1] it was suggested, on the basis of electronic spectra and electrochemical data for the iron(II) complexes, that there is a significant measure of metal(d_{xz}, d_{yz})–macrocycle(p_{π^*}) charge-transfer.

Of the six resonance forms, the Fe–N(pyridine) double-bond occurs twice and the Fe–N(imino) double bond once (for each of these bonds). No double bonding is possible, of course, to the saturated nitrogens of the macrocycle. Thus we have a predicted relative bond-length order, in agreement with observation.

It would appear, then, that when the oxidation state of the metal is reduced from +3 to +2 there is a small but significant change in metal–macrocycle bonding, such that the metal moves relatively closer to the unsaturated segment of the macrocycle. These observations provide strong support for our assignment of electronic spectra.[1] Moreover, the greater (structural) effect found for the L^1 compared to the L^2 complexes is in complete accord with the metal–macrocycle charge-transfer band in the iron(II) macrocycle, L^2 complexes being of higher energy. The theory is further supported by the observation that when the axial NCS^- ligands are replaced by H_2O, in $[FeL^1(H_2O)_2]Cl\cdot ClO_4$, the Fe–N(pyridine) distance increases by a significant extent (0.061 Å).[3] This increase is once again in accord with expectation since in the diaqua-complex the metal macrocycle charge-transfer absorption occurs at appreciably higher energy.[1]

The metal–thiocyanate bond angles in (I) and (II) are significantly less than 180° and are similar to those found in (III) being in the range 153—168°; the angles in (IV) are smaller (*ca.* 140°). In structures containing the thiocyanate ion bonded to a metal atom through nitrogen, a wide range of angles have been obtained, ranging from 129° (ref. 9) up to 180°, though the majority of examples fall in the range 150—180°.[10] It has been suggested that inter- and intra-molecular forces affect this angle though such effects are difficult to prove; however, see ref. 11 for a notable example. In the present complexes, there is no obvious steric reason for the non-linear arrangements, and electronic effects should therefore be considered. Two resonance structures (V) and (VI) for isothiocyanate–metal complexes, representing, respectively linear and non-linear bonding, may be written. Since linear *N*-bonded $[NCS]^-$ is a potential acceptor of π-electrons we suggest that the occurrence of the bent form (VI) in the present complexes is a consequence of the non-availability of the metal d_π electrons, which, as already stated, are involved in π-overlap with the macrocycle.

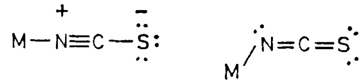

(V) (VI)

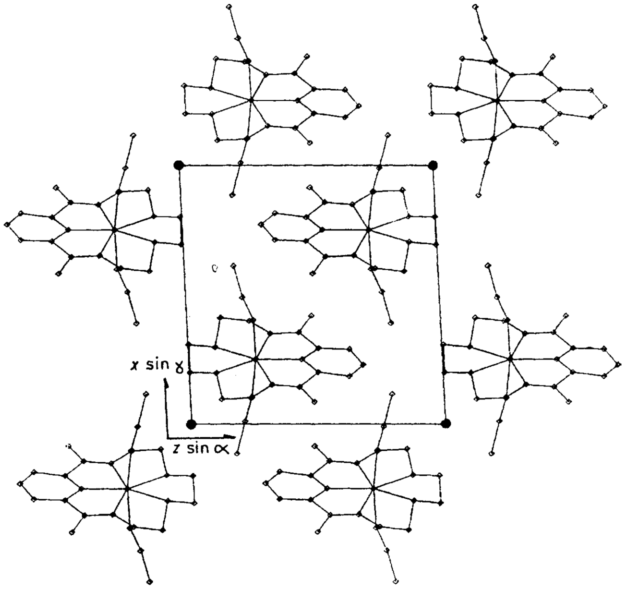

FIGURE 3 The unit cell of (I) in the *b* projection

A detailed account of the conformations of macrocycles L^1 and L^2 is given in ref. 2 and so only a few details

---

[9] J. Korvenranta and A. Pajunen, *Suomen Kem.*, 1970, **B43**, 119.

[10] M. G. B. Drew and A. H. Othman, *Acta Cryst.*, 1975, **B31**, 613.

[11] D. V. Naik and W. R. Scheidt, *Inorg. Chem.*, 1973, **12**, 273.

will be given here. The angles subtended at the metal in the equatorial plane are slightly different in (I) and (III); in (I) N(6)–Fe–N(9) and N(9)–Fe–N(12) are increased slightly, presumably to increase the N(6) · · ·N(9) and N(9) · · · N(12) contacts. The distortion in (II) from the C_2 symmetry found in (I) is similar to that in (IV), Fe–N(3) being 0.05 Å longer than Fe–N(15), and this has been shown to be related to the chair conformation of the six-membered ring. As in (IV), C(5) is further from the equatorial plane than C(13). The angles subtended at N(3) and N(15) follow the same pattern in (II) and (IV). The conformations of the saturated rings in (I) and (II) are equivalent to those in (III) and (IV). It is noticeable that the conformations of the rings in (I) are remarkably close to C_2 symmetry. The changes in Fe–N bond lengths from macrocycle L^1 to L^2 are similar but not equivalent for the Fe^{II} and Fe^{III} complexes (see Table 6), thus demonstrating that for these four molecules Fe–N bond lengths are dependent upon a complicated mixture of electronic and steric effects.

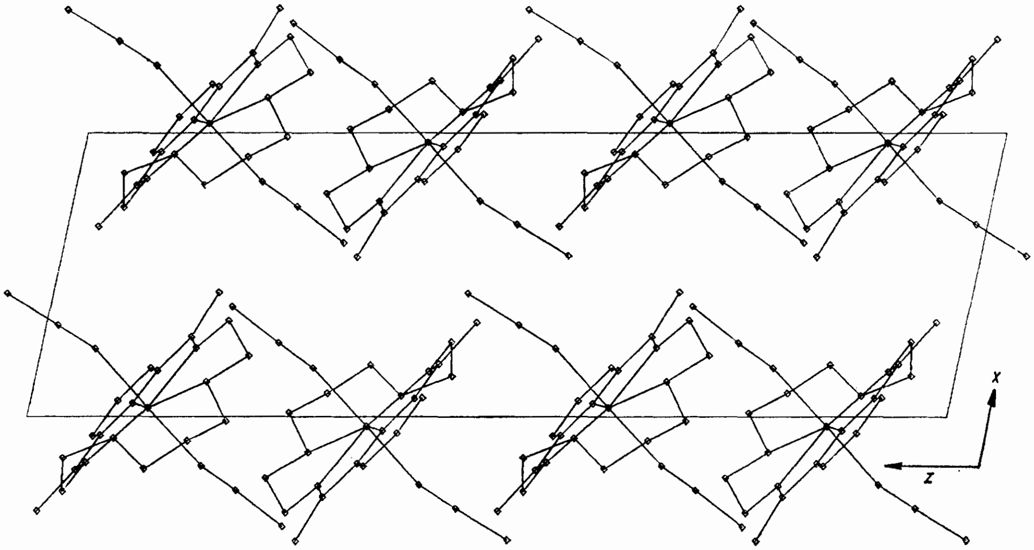

FIGURE 4 The unit cell of (II) in the *b* projection

The packing of the molecules in (II) seems more efficient than that found in the triclinic (I) as seen for the greater number of short contacts and the density larger by *ca.* 7%. The two unit cells, both in the *b* projections, are shown in Figures 3 and 4.

We thank the National University of Malaysia for a grant (to A. H. O.) and A. W. Johans for his assistance with the crystallographic investigations.

[5/1723 *Received, 8th September,* 1975]